PNAS RESEARCH ARTICLE | MICROBIOLOGY

Reconstitution of a biofilm adhesin system from a sulfate-reducing bacterium in *Pseudomonas fluorescens*

Amruta A. Karbelkar[a], Maria Font[b], T. Jarrod Smith[a], Holger Sondermann[b], and George A. O'Toole[a,1]

Edited by John Mekalanos, Harvard University, Boston, MA; received November 20, 2023; accepted February 21, 2024

Biofilms of sulfate-reducing bacterium (SRB) like *Desulfovibrio vulgaris* Hildenborough (DvH) can facilitate metal corrosion in various industrial and environmental settings leading to substantial economic losses. Although the mechanisms of biofilm formation by DvH are not yet well understood, recent studies indicate the large adhesin, DvhA, is a key determinant of biofilm formation. The *dvhA* gene neighborhood resembles the biofilm-regulating Lap system of *Pseudomonas fluorescens* but is curiously missing the c-di-GMP-binding regulator LapD. Instead, DvH encodes an evolutionarily unrelated c-di-GMP-binding protein (DVU1020) that we hypothesized is functionally analogous to LapD. To study this unusual Lap system and overcome experimental limitations with the slow-growing anaerobe DvH, we reconstituted its predicted SRB Lap system in a *P. fluorescens* strain lacking its native Lap regulatory components (Δ*lapG*Δ*lapD*). Our data support the model that DvhA is a cell surface–associated LapA-like adhesin with a N-terminal "retention module" and that DvhA is released from the cell surface upon cleavage by the LapG-like protease DvhG. Further, we demonstrate DVU1020 (named here DvhD) represents a distinct class of c-di-GMP-binding, biofilm-regulating proteins that regulates DvhG activity in response to intracellular levels of this second messenger. This study provides insight into the key players responsible for biofilm formation by DvH, thereby expanding our understanding of Lap-like systems.

Lap system | RTX adhesion | sulfate-reducing bacterium | *Pseudomonas fluorescens*

Significance

Corrosion leads to ~2.5 trillion US dollars in economic losses, 20% of which are estimated to be microbially induced. Biofilms of sulfate-reducing bacteria (SRB), especially the genus *Desulfovibrio*, are important members of the corrosion consortium and accelerate deterioration of metals. Understanding how biofilms are formed by SRB can provide important clues to mitigate this challenge. In this study, we used genetic and biochemical tools to investigate the mechanism of biofilm formation by *Desulfovibrio vulgaris* Hildenborough. Our study reveals critical genes responsible for regulating the secretion of a large adhesin known to be required for biofilm formation and lays the groundwork for engineering bacteria to control their ability to form a biofilm.

Bacteria predominantly exist as biofilms in various environmental niches (1). Free-swimming bacteria can sense diverse inputs and respond to those cues by transitioning to surface-attached biofilms (2). Initial steps in biofilm formation require various factors, including flagella, pili and protein adhesins, and exopolysaccharides (2). Biofilms eventually become embedded in an adhesive matrix consisting of polysaccharides, proteins, and extracellular DNA (3). While the triggers and mechanisms of biofilm formation are varied among different bacteria, these processes are ultimately governed by bacterial nucleotide secondary messenger c-di-GMP in many microbes (4).

Biofilms of sulfate-reducing bacteria (SRB), particularly of the genus *Desulfovibrio*, have been shown to play an important role in bioremediation of heavy metals (5) and sulfur cycling in various ecological settings (6). These microbes can accept electrons from extracellular electron donors, such as minerals or electrodes (7). As a result, their biofilms can be used as catalysts in bioelectrochemical systems for wastewater treatment (8) and energy production (9). SRB are also responsible for substantial economic losses as their biofilms can clog gas and oil pipelines and cause microbially induced corrosion of metal structures (10). Therefore, understanding SRB biofilms and how they form has major implications for both natural and engineered systems.

The gram-negative, obligate anaerobe, *Desulfovibrio vulgaris* Hildenborough has been used as a model organism to understand the mechanisms and effects of biofilm formation by SRB (11). For example, quorum sensing affects various metabolic processes of *D. vulgaris* including an increase in biofilm formation (12). Several studies have also investigated the components of biofilm matrix. For example, analysis of gene expression levels in *D. vulgaris* biofilms showed up to a 1.8-fold increase in exopolysaccharide biosynthesis gene expression compared to planktonic cells (13). The biofilm matrix of *D. vulgaris* has been shown to be protein-rich (observed as filaments by electron microscopy) and low in carbohydrates (14). Transcriptomic and proteomic analysis of *D. vulgaris* biofilms revealed two large proteins, DVU1012 and DVU1545, in the biofilm matrix, both of which contribute to biofilm formation (15). Isolation and identification of membrane-associated proteins implicated DVU1012 as being localized to the outer membrane in two separate studies (16, 17). More recently, a study focusing on a *D. vulgaris* variant that unexpectedly lost its ability to form a biofilm discovered that a spontaneous mutation in an ABC transporter component DVU1017 was responsible for this phenotype. Incidentally, the DVU1017 protein is situated several genes downstream of the gene coding for the large protein

Author affiliations: [a]Department of Microbiology and Immunology, Geisel School of Medicine at Dartmouth, Hanover, NH 03755; and [b]CSSB Centre for Structural Systems Biology, Deutsches Elektronen-Synchrotron DESY, D-22607 Hamburg, Germany

Author contributions: A.A.K., M.F., H.S., and G.A.O. designed research; A.A.K., M.F., and T.J.S. performed research; A.A.K., M.F., T.J.S., H.S., and G.A.O. analyzed data; and A.A.K., M.F., H.S., and G.A.O. wrote the paper.

The authors declare no competing interest.

This article is a PNAS Direct Submission.

[1]To whom correspondence may be addressed. Email: georgeo@dartmouth.edu.

This article contains supporting information online at https://www.pnas.org/lookup/suppl/doi:10.1073/pnas.2320410121/-/DCSupplemental.

Published March 18, 2024.

DVU1012 (18). This study strongly suggested that DVU1017 is part of a non-canonical type I secretion system (T1SS), called the Lap system (19), that has been thoroughly characterized for its role in biofilm formation in the environmental microbe *Pseudomonas fluorescens* Pf0-1. That is, DVU1012 was proposed to be the LapA-like protein of *D. vulgaris* (18).

Biofilm formation by *P. fluorescens* Pf0-1 is mediated primarily by a large adhesive protein, LapA which is localized to the outer membrane via anchoring in the LapE outer membrane protein (Fig. 1*A*) (20). The Lap system is composed of an ABC-transporter LapB, fusion protein LapC, and outer membrane TolC-like LapE that allows LapA to traverse from the cytoplasm to the outer membrane via its C-terminal secretion domain. Our previous biochemical studies and comparison to the N terminus of another LapA-like protein from an ice-binding bacterium (21) indicate that the N terminus of LapA can fold into a retention module (RM) which allows LapA to remain anchored to the OM (22). LapA displayed on the outer membrane allows cells to adhere to a surface and promote biofilm formation. Whether LapA remains tethered to the OM depends upon two regulatory proteins: a periplasmic protease LapG and an effector protein LapD, the latter of which can bind c-di-GMP via its catalytically inactivate c-di-GMP phosphodiesterase "EAL" domain (23, 24). The LapG protease can cleave LapA downstream of the retention module leading to a loss of the adhesin from the cell surface. Under conditions of high intracellular c-di-GMP, this cyclic dinucleotide binds to the cytoplasmic EAL domain of LapD, which in turn leads to sequestration of LapG in a LapD-LapG complex in the periplasm. As a result, LapA remains tethered to the OM. Under low c-di-GMP conditions, this second messenger is not available for LapD binding, and this receptor undergoes a conformational change allowing the release of LapG in the periplasm (Fig. 1*A*). LapG then cleaves LapA, causing release of LapA and a loss of the biofilm (23, 25).

In this study, we build on a bioinformatic analysis that revealed an unusual Lap-like system in *D. vulgaris* Hildenborough. We investigate the mechanism of biofilm formation mediated by the Lap-like system of *D. vulgaris* via heterologous expression of introduce components of the SRB Lap system into *P. fluorescens* Pf0-1. This analysis provides insight into a group of Lap-like adhesion systems distinct from those found in gammaproteobacteria.

Results

Bioinformatic Analysis Suggests a Distinct Class of Lap-Like Biofilm Systems in SRBs. To date, our knowledge of how cell surface levels of LapA-like adhesins are regulated arises from work done largely in fluorescent pseudomonads, including *P. fluorescens* Pf0-1 (abbreviated here as Pf0-1) with some additional studies in *Bordetella bronchiseptica*, *Legionella pneumophila,* and *Vibrio cholerae* (26–29). LapG and LapD regulatory proteins can be bioinformatically identified by the presence of a C93 Peptidase Domain (LapG) and N-terminal LapD_MoxY_N domain (LapD) and thus used to define genomes likely encoding the Lap system. While surveying the distribution of bacterial genomes with Lap components, we noted several genera that encoded LapG-like proteins but no clear LapD-like regulator (*SI Appendix*, Fig. S1*A*), including sulfur-reducing bacteria (SRBs) like *Desulfovibrio* (*SI Appendix*, Fig. S1*B*). We suspected these orphan LapG-like proteins might be regulated by a yet unknown mechanism and perhaps represent a class of Lap systems distinct from those reported for gammaproteobacteria.

Manual inspection of the genes surrounding the bioinformatically identified *lapG* gene of several SRBs, including *D. vulgaris* Hildenborough revealed genetic architecture similar to the Lap system of *P. fluorescens* (*SI Appendix*, Fig. S1*C*), including a large adhesin (DVU1012, *dvhA*) and its putative transport machinery (DVU1013, DVU1017, DVU1018; DvhEBC), but no clear *lapD* homolog (18) (*SI Appendix*, Fig. S1*C*). The gene next to the LapG-like protein of DvH (DVU1019, DvhG), DVU1020, does not share any sequence or domain similarity with LapD but contains analogous domains that may allow it to regulate DvhG activity via a mechanism analogous to LapD regulation of LapG. We thus renamed DVU1020 to DvhD as detailed below. While LapD binds c-di-GMP using a catalytically inactive cyclic diguanylate phosphodiesterase EAL domain and LapG through its periplasmic LapD_MoxY_N domain, DvhD contains a HDc diguanylate phosphodiesterase domain that is predicted to be catalytically inactive and a large periplasmic region that could potentially interact with DvhG (Fig. 1*B*).

Proposed Model of Biofilm Regulation by the Non-Canonical SRB Lap System. While performing the bioinformatic analysis outlined above, De León et al. reported functional data supporting a role for the DvhABCE system in biofilm formation (18). Specifically, a spontaneous point mutation arose in the *dvhB* gene (coding for a component of the T1SS) rendering the strain biofilm-defective and with no detectable DvhA on the surface of the cell. Based on our bioinformatic analysis and study of the Pf0-1 Lap system, the work from De León et al. (18) suggests cell surface regulation of DvhA by *D. vulgaris* may represent class of Lap biofilm regulatory system distinct from those previous described in gammaproteobacteria.

In this model (Fig. 1*B*), we hypothesize that DvhA can be translocated from the cytoplasm to the OM via the components of the T1SS: DvhB, DvhC, and DvhE. The N terminus of the DvhA sequence has spaced glycine residues that suggest possible folding into a retention module as observed for LapA (*SI Appendix*, Figs. S1*D* and S2*A*). DvhA also possesses an N-terminal di-alanine motif (106AA107) characteristic of LapA-like adhesins and essential for LapG proteolysis in *P. fluorescens* Pf0-1 (30), that likely serves at the DvhG cleavage site. DvHA also has several domains predicted to be localized outside the outer member, including two repeat domains rich in β-sheets, a von Willebrand type A domain and a predicted C-terminal Serralysin-like metalloprotease domain (*SI Appendix*, Fig. S2*B*).

Interestingly, the DvhG sequence reveals a transmembrane helix (Fig. 1*B*), which suggests that this protease is periplasmic but anchored in the inner membrane, unlike LapG which is free-floating in the periplasm. DvhD is a predicted inner membrane-bound protein which has a periplasmic domain and a cytoplasmic PAS domain fused with a phosphodiesterase (PDE) "HD-GYP"-like domain that, based on the lack of key residues, is predicted to be catalytically inactive (31). LapD, in contrast, is composed of a periplasmic PAS domain, a cytoplasmic HAMP domain with catalytically inactive DGC "GGDEF" and PDE "EAL" domain, the latter of which can bind c-di-GMP (*SI Appendix*, Fig. S2*C*) (25). While the domains of LapD and DvhD proteins are distinct, we predicted that DvhD may be functionally analogous to LapD since they both have periplasmic and cytoplasmic signaling domains that are fused to inactive PDE domains. Thus, we predicted that DvhD can drive signaling through c-di-GMP binding. Overall, our model proposes that DvhG and DvhD can regulate localization of the large adhesin DvhA via c-di-GMP in a manner analogous to LapD/LapG (Fig. 1*B*).

To test the model above, we sought to heterologously express the *D. vulgaris* Lap components in a Pf0-1 background lacking its native LapD and LapG. We decided on this approach for the following reasons: 1) While tools for genetic manipulation have been developed for this SRB (32–34), *D. vulgaris* is an obligate anaerobe and is difficult to culture and genetically manipulate

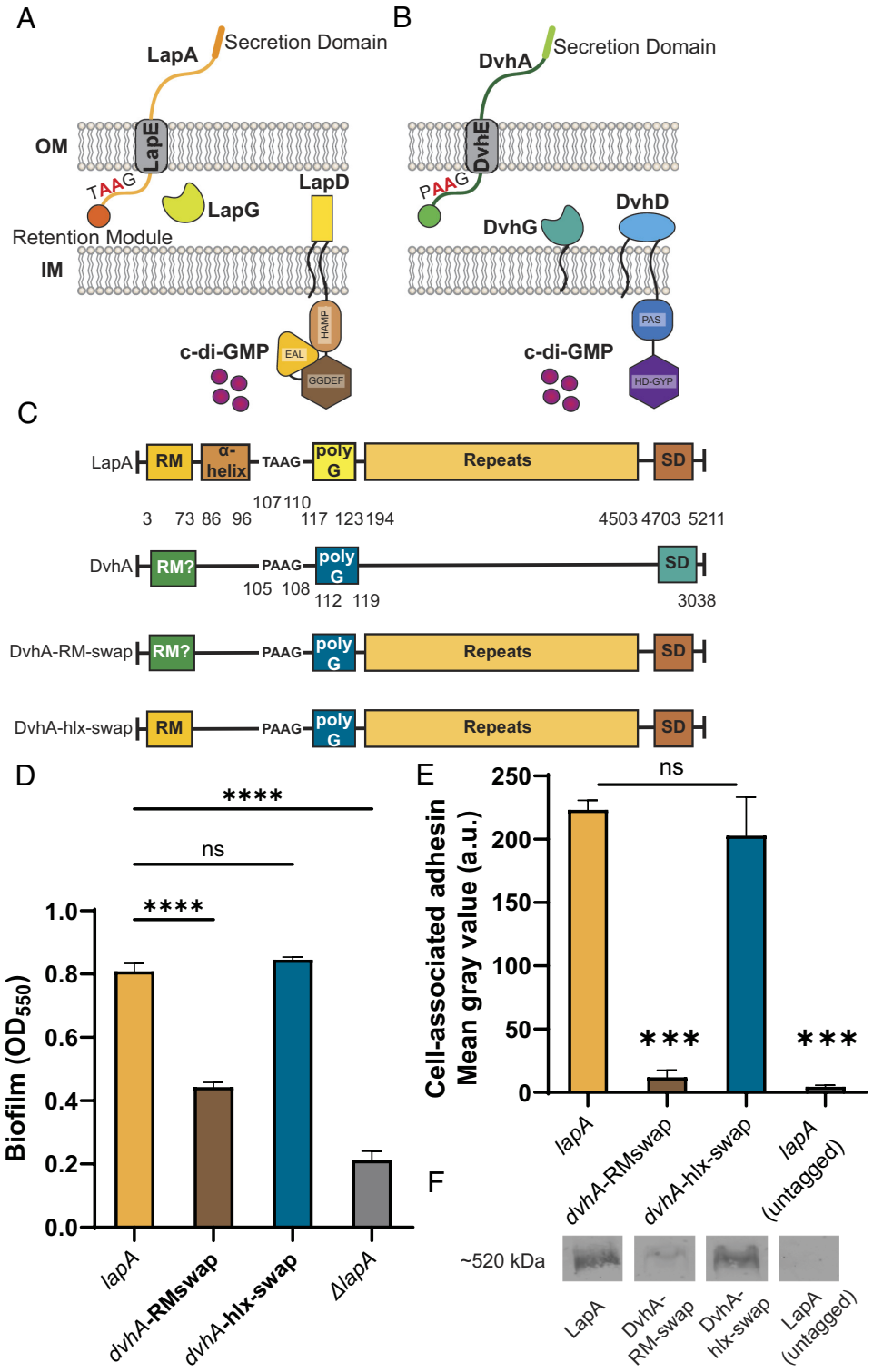

Fig. 1. Simplified model of two-step Type 1 secretion system (T1SS). (*A*) T1SS in *P. fluorescens* Pf0-1. The large adhesin LapA is localized to the outer membrane (OM) via a retention module, allowing the bacterium to form a biofilm. The localization of LapA to the OM is regulated by a periplasmic protease LapG and a cyclic di-GMP (cdG) effector protein LapD. At high intracellular cdG levels, the catalytically inactive EAL domain of LapD binds cdG leading to a conformational change whereby the LapD periplasmic domain sequesters LapG, thereby retaining LapA on the OM. When c-di-GMP levels are low, LapD is in its autoinhibited conformation (as shown here), which releases LapG to cleave LapA at a di-alanine motif (shown in red), resulting in the release of LapA to the extracellular environment and loss of biofilm formation. (*B*) Proposed model of T1SS in *D. vulgaris* Hildenborough. DvhA is a LapA-like adhesin localized to the OM. DvhG is a LapG-like protease that can cleave DvhA at the di-alanine site (shown in red), however, unlike the periplasmic-localized LapG, DvhG is hypothesized to be inner membrane (IM) bound. DvhD is a structurally different but functionally analogous LapD-like protein containing a catalytically inactive HD-GYP domain that can bind c-di-GMP and thus regulate DvhA localization and biofilm formation by *D. vulgaris* Hildenborough. (*C*) Simplified protein architecture representing different domains and the di-alanine site of Pf0-1 adhesin LapA, DvH adhesin DvhA and fusion proteins DvhA-RM-swap and DvhA-hlx-swap (RM-retention module; hlx-helix; polyG-polyglycine linker; SD – C-terminal secretion domain). Protein domains are not to scale. (*D*) Biofilm formed in K10T medium at 24 h for strains expressing the adhesins DvhA-RM-swap and DvhA-hlx-swap compared to the native adhesin LapA in Pf0-1 and the Δ*lapA* mutant, all in the Δ*lapG*Δ*lapD* background strain. (*E*) Quantification of cell surface levels of HA-tagged adhesins at 24 h in K10T medium for the indicated strains. (*F*) Western blots indicating total cellular levels of the different adhesins. Statistical analysis was performed using one-way ANOVA corrected for multiple comparisons (ns, $P > 0.05$; *$P \leq 0.05$; **$P \leq 0.01$; ***$P \leq 0.001$; ****$P \leq 0.0001$; ****$P < 0.0001$).

compared to Pf0-1, and 2) Our lab has extensively studied the Pf0-1 Lap system, and thus we have a large battery of background strains, cloning tools, and experimental systems that could be deployed to understand the *D. vulgaris* Lap system.

The N terminus of DvhA Functions as a Retention Module That Promotes Biofilm Formation. DvhA is a 3,038-aa protein that consists of calcium-binding, von Willebrand factor, and glycine-rich domains which are commonly found in LapA-like proteins (Fig. 1*C* and *SI Appendix*, Fig. S2*B*) (20). The N terminus of DvhA resembles the beta-helical N-terminal retention module domain of LapA (*SI Appendix*, Figs. S1*D* and S2 *A* and *B*). Hence, we hypothesized DvhA's N terminus folds into a retention module required for biofilm formation. The large size *dvhA*'s ORF (~9.2 kb) makes it challenging to clone and express in a heterologous system. Since we previously demonstrated that the retention modules of LapA-like proteins are largely interchangeable (22), we replaced RM of LapA (M1-125S) with the predicted RM of DvhA (M1-119G). We used this chimera, called "DvhA-RM-swap" (Fig. 1*C*) to test whether DvhA's N terminus can support cell surface localization of LapA.

DvhA-RM-swap was introduced into the Δ*lapG*Δ*lapD* genetic background for two reasons: 1) Lack of a functional LapG should result in stoichiometric retention of the fusion proteins on the outer membrane (35), and 2) this strain background would allow us to introduce the DvhG/DvhD proteins to assess their function in the context of the fusion protein.

To test whether the N terminus of DvhA functions as a retention module, we performed a static biofilm assay with DvhA-RM-swap strain at 24 h and compared the extent of biofilm formation to the WT Pf0-1 strain expressing LapA as a positive control and no LapA (Δ*lapA*) as a negative control. Our results indicate that DvhA-RM-swap fusion protein can promote biofilm formation (Fig. 1*D*), and although these biofilms were less robust than the WT Pf0-1, they were significantly higher than the negative control (OD_{550} = 0.45 ± 0.008 vs. 0.21 ± 0.02, P = 0.0002).

To assess whether the differences in biofilm formation by the strain producing the DvhA-RM-swap variant were due to different amounts of adhesins localized to the cell surface, we performed dot blots using a hemagglutinin (HA) tag that was previously engineered into the chromosome of the gene encoding LapA (36). Cells were grown for 24 h, centrifuged, washed, and OD_{600} normalized before spotting directly on a nitrocellulose membrane. Upon imaging the membrane and quantifying the intensity of the spots, we found that there was significantly less DvhA-RM-swap fusion protein on the cell surface compared to LapA (Fig. 1*E*). This reduced cell-surface DvhA-RM-swap fusion protein was likely due to the fact that the DvhA-RM-swap fusion protein was unstable (Intensity = 1.85 ± 0.36 × 10^3 a.u.; Fig. 1*F*). The amount of surface localized fusion protein was not significantly different from the negative control; however, it trends higher (Mean gray value = 18.5 ± 3.97 vs. 10.2 ± 1.97, P = 0.098; Fig. 1*E*). Together, these data indicate that the N-terminal portion of DvhA can serve to anchor LapA to the cell surface to promote biofilm formation, although this fusion protein is unstable.

Because DvhA-RM-swap fusion protein was unstable, we tested a second fusion protein, where we replaced the residues in LapA shown to be critical for LapG processing (A81-123G) with the corresponding region of DvhA (G87-119G), for its stability and function. This fusion, called DvhA-hlx-swap, was similarly constructed in the Pf0-1 Δ*lapG*Δ*lapD* background (Fig. 1*C*). To determine the ability of the DvhA-hlx-swap fusion protein to support biofilm formation, we performed a static biofilm assay. The DvhA-hlx-swap (OD_{550} = 0.84 ± 0.005) strain formed a biofilm similar to Pf0-1 expressing WT LapA (OD_{550} = 0.80 ± 0.01; Fig. 1*D*) and dot blot analysis to probe for surface-associated adhesin revealed no difference in signal for the DvhA-hlx-swap fusion and LapA (Fig. 1*E*). Western blotting for cytoplasmic LapA and the DvhA-hlx-swap fusion found equivalent signal for LapA and DvhA-hlx-swap fusion (Intensity = 16.3 ± 1.9 × 10^3 a.u. vs. 16.5 ± 0.45 × 10^3 a.u.; P > 0.05) (Fig. 1*F*).

We confirmed the DvhA-hlx-swap fusion uses LapA's T1SS machinery by deleting the ABC transporter, *lapB,* which significantly reduced the biofilm formed and eliminated our ability to detect cell surface–associated adhesin (*SI Appendix*, Fig. S3 *A* and *B*). Given the comparable stability of DvhA-hlx-swap to LapA, we decided to explore the mechanism of *D. vulgaris* Lap-like system using the Pf0-1 Δ*lapG*Δ*lapD* genetic background expressing the DvhA-hlx-swap variant in all the experiments described below.

DvhG Can Cleave the Fusion Adhesin DvhA-hlx-swap. LapG is a bacterial transglutaminase-like cysteine protease (BTLCP) that cleaves LapA at a 108AA109 di-alanine motif (35, 37). This proteolysis occurs in the periplasm and removes the N-terminal retention module of LapA, allowing cleaved LapA to "slip" out of the outer membrane LapE channel, thereby leading to a loss of cell surface–associated LapA and LapA-mediated adhesion. Thus, based on this information, we would predict that DvhG functions similarly to Pf0-1 LapG because 1) DvhG also belongs to the BTLCP family of proteins (*SI Appendix*, Fig. S4) and 2) the adhesin DvhA possesses a di-alanine motif at 106AA107 that could serve as a proteolytic site for DvhG (*SI Appendix*, Fig. S1*D*).

First, to test whether DvhG can cleave DvhA-hlx-swap and reduce biofilm formation in this strain, we cloned *dvhG* carrying an N-terminal 6-His tag into the arabinose-inducible multicopy plasmid pMQ72 (pMQ72-*dvhG*). The P_{BAD} promoter is known to exhibit leaky expression in the absence of induction and can often complement mutant strains without inducer present (38). This plasmid was then transformed into the Pf0-1 Δ*lapG*Δ*lapD dvhA-hlx-swap* strain. Static biofilm assays were performed in the absence or presence of the inducer, 0.2% arabinose, for 24 h. The same background strain harboring the pMQ72 plasmid, which we refer to as the empty vector (EV) control, or a strain lacking any plasmid were used as negative controls. The presence of DvhG dramatically decreased biofilm formation compared to the EV control strain (Fig. 2*A*) in the presence or absence of arabinose, indicating leaky expression was sufficient to generate a measurable impact of DvhG activity. Western blot analysis indicates the DvhG protein is stably expressed (Fig. 2*B*). Consistent with our model, a decrease in biofilm formation corresponded with decreased levels of DvhA-hlx-swap protein at the cell surface (Fig. 2*C*) and increased levels in the supernatant (Fig. 2*D*). Taken together, these data suggest that DvhG likely serves as a key regulator of DvH biofilm formation.

Studies from our lab previously demonstrated that mutating LapA's di-alanine motif (A108-109A) to di-arginine residues largely blocks LapG cleavage (30), with low levels of cleavage likely occurring at nearby di-alanine or di-alanine-like sites (*SI Appendix*, Fig. S1*D*). To further test our model that DvhG cleaves DvhA at a similar di-alanine site, we similarly mutated the corresponding di-alanine residues (A106-107A) in the DvhA-hlx-swap strain to di-arginine residues. We then compared biofilm formation of the DvhA-hlx-swap and di-alanine mutant DvhA-hlx-swap AA-RR in strains carrying pMQ72-*dvhG* plasmid or empty vector after 24 h with and without arabinose induction (*SI Appendix*, Fig. S5*A*). Under inducing and non-inducing conditions, the DvhA-hlx-swap AA-RR mutant is more resistant to DvhG proteolysis, suggesting like LapG, DvhG cleaves its cognate adhesin DvhA at a di-alanine site. Without arabinose induction of DvhG, the DvhA-hlx-swap AA-RR mutant forms biofilms similarly to

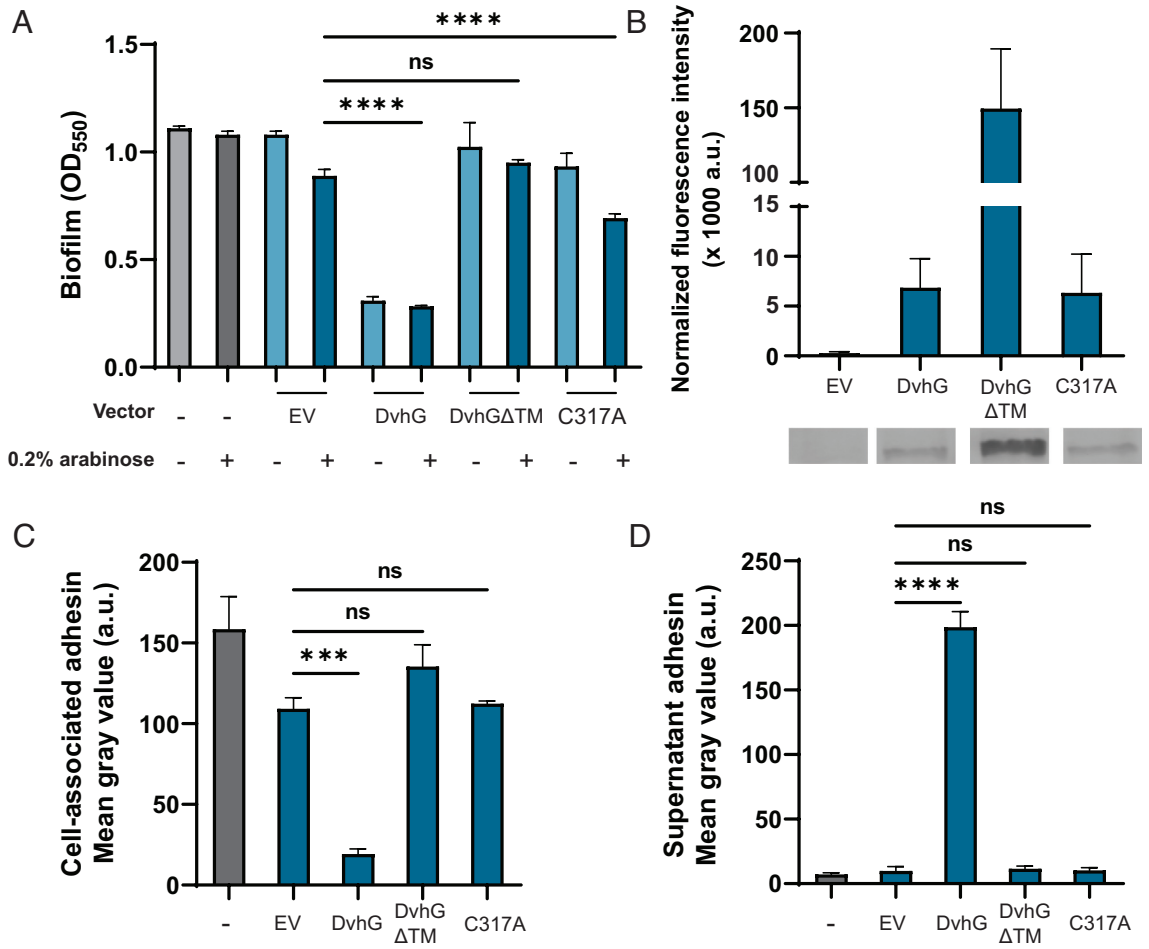

Fig. 2. DvhG can cleave DvhA-hlx-swap protein and diminish biofilm formation. The gene encoding His-tagged DvhG and its variants were cloned in an arabinose inducible promoter and transformed into Pf0-1 *ΔlapGΔlapDdvhA-hlx-swap* strain. The protease was induced with 0.2% arabinose. (*A*) Biofilm formed in K10T medium at 24 h in the presence or absence of arabinose with no vector, empty vector (EV), or a plasmid expressing full-length DvhG, DvhG lacking the predicted transmembrane helix domain (DvhGΔTM) or DvhG with mutated catalytic residue (C317A). (*B*) Quantification of DvhG and the mutated protein levels normalized to total protein loaded. Bars and error bars represent mean and SEM for three biological replicates. Representative western blot images are displayed underneath the bar plot corresponding to the DvhG variants. (*C*) Cell surface levels of DvhA-hlx-swap in the presence of 0.2% arabinose. (*D*) DvhA-hlx-swap levels in the culture supernatants at 24 h in the presence of 0.2% arabinose. Statistical analysis was performed using one-way ANOVA corrected for multiple comparisons (ns, $P > 0.05$; *$P \leq 0.05$; **$P \leq 0.01$; ***$P \leq 0.001$; ****$P \leq 0.0001$).

EV control strain (OD_{550} = 0.64 ± 0.08). Upon increasing the level of DvhG by arabinose induction, we see a decrease in biofilm formation (OD_{550} = 0.40 ± 0.13, P = 0.06; *SI Appendix*, Fig. S5*A*), but still above the level of the biofilm formed for a strain carrying the DvhA-hlx-swap with the AA proteolysis site and expressing DvhG (OD_{550} = 0.30 ± 0.03; Fig. 2*A*; this level is also represented by the dashed line in *SI Appendix*, Fig. S5*A*). In agreement with the biofilm data, in the presence of DvhG, we observed 65% more localization of DvhA-hlx-swap AA-RR on the cell surface and 32% less accumulation in the supernatant than DvhA-hlx-swap with the native AA motif (Fig. 2*D* and *SI Appendix*, Fig. S5 *B* and *C*), suggesting that the mutated adhesin was not processed as efficiently as DvhA-hlx-swap with the WT proteolysis site.

Overall, using multiple lines of evidence, we show that the N terminus of DvhA has a retention module that allows localization of the fusion protein to the cell surface, thereby promoting biofilm formation, and that the DvhG-mediated proteolysis at the DvhA-hlx-swap di-alanine motif releases this adhesin from the surface, thereby reducing biofilm formation.

The Role of the Predicted Transmembrane Domain of DvhG. Unlike LapG, which is a periplasmic protease, DvhG has a predicted transmembrane (TM) helix suggesting that this protease may be inner membrane bound, with the catalytic domain localized to the periplasm. To assess whether the TM helix is essential for DvhG proteolytic activity, we cloned *dvhG* lacking the TM helix (deletion of aa 1 to 40; called *dvhG*ΔTM) with an N-terminal 6×-His tag, into the pMQ72 plasmid (pMQ72-*dvhG*ΔTM). Upon transforming this plasmid into Pf0-1Δ*lapG*Δ*lapD dvhA-hlx-swap* strain and testing for its ability to form biofilms, we found that this strain was not significantly different from the empty vector control even in the presence of arabinose (OD_{550} = 0.95 ± 0.02 vs. 1.02 ± 0.2; Fig. 2*A*), despite DvhGΔTM protein being more stable than WT DvhG (Intensity = 149.4 ± 40.0 × 10^3 a.u; Fig. 2*B*). Supporting the biofilm findings, the level of the DvhA-hlx-swap protein on the cell surface and supernatant for the strain expressing DvhGΔTM was not significantly different from the controls (Fig. 2 *C* and *D*). Together, these data indicate the TM helix is essential for DvhG to process/recognize DvhA and point to a layer of regulation not found in well-described Lap systems.

The finding above that without its TM helix DvhG cannot cleave DvhA-hlx-swap could be explained by 1) the fact that in the absence of the TM helix the protein is unstable in the periplasm and/or 2) the inability of the variant TM-less DvhG to properly localize to the periplasm. Therefore, collectively our findings suggest that the lack of proteolytic activity is likely due to the

inability of the variant to access the AA motif downstream of the N-terminal retention module adhesin in the periplasm.

DvhG Requires Catalytically Active Cysteine Residue to Function. Multiple sequence alignment analysis comparing DvhG with LapG-like proteases showed conserved cysteine, histidine, and aspartate (C-H-D) triad that has previously been shown essential for LapG activity (*SI Appendix*, Fig. S4). To test the importance of the cysteine residue of DvhG, we mutated this residue to alanine (C317A) and cloned the full-length mutated *dvhG* into the arabinose-inducible pMQ72 plasmid (pMQ72-*dvhG*-C317A). This plasmid was transformed into Pf0-1Δ*lapG*Δ*lapD dvhA-hlx-swap* strain and we compared the biofilm formed, and whole cell and surface levels of the DvhA-hlx-swap protein to the strains containing WT DvhG or the EV.

We performed static biofilm assays with these strains in K10T-1 medium at 24 h with and without 0.2% arabinose inducer (Fig. 2*A*). As expected, the strain expressing DvhG showed reduced biofilm formation when compared to the EV control regardless of the inducer. In contrast, the strain expressing the DvhG-C317A mutant forms a biofilm equivalent to that of the EV control under non-inducing conditions ($P = 0.88$). With arabinose, DvhG-C317A displays a modest but significant reduction ($OD_{550} = 0.69 \pm 0.03$) in biofilm formation compared to the EV control ($OD_{550} = 0.89 \pm 0.05$); however, these biofilms are still significantly higher than strain expressing WT DvhG ($P < 0.0001$). A western blot shows the DvhG-C317A protein variant is as stable of the WT DvhG (Intensity = $6.35 \pm 3.8 \times 10^3$ a.u.; Fig. 2*B*). Dot blots also show comparably high levels of DvhA-hlx-swap on the cell surface of EV and DvhG-C317A mutant strain and low levels of the adhesin in their respective supernatants, compared to the strain expressing the WT DvhG (Fig. 2 *C* and *D*).

Our previous studies showed that LapG activity requires calcium ions, consistent with the observation that the structure of LapG contains several calcium ions (29, 35). We also note conserved calcium-binding residues in the sequence of DvhG (*SI Appendix*, Fig. S4) and observe calcium-dependence of DvhG function in vivo (*SI Appendix*, Fig. S5 *D–F*). Finally, we assessed the ability of LapG to target LapA versus the DvhA-hlx-swap fusion protein, and for DvhG to target these two substrates. These results show that these proteases are proficient in processing their own adhesins but less efficient toward the other adhesins (*SI Appendix*, Fig. S6). Together, these data suggest that the cysteine residue and calcium binding of DvhG are critical for its proteolytic activity and that each protease has preference for its cognate proteolysis site.

DvhD Regulates DvhG Cleavage of DvhA. While DvhA and DvhG resemble LapA and LapG of the Lap system, respectively, we were unable to find a protein encoded by DvH that contained the periplasmic LapD_MoxY_N and catalytically inactive cytoplasmic EAL domains that define LapD-like proteins. However, the gene next to *dvhG*, DVU1020, contains analogous features of LapD, such as a large periplasmic region that might interact with DvhG and a catalytically inactive HDc domain that, like catalytically inactive EAL domains, can act as c-di-GMP receptors. To test the idea that DVU1020 possesses LapD-like activity and can regulate DvhG cleavage of DvhG, we next asked whether DVU1020 expression can increase biofilm formation in the DvhA-hlx-swap strain expressing DvhG. To perform this experiment, we cloned DVU1020 containing a HA-tag under an IPTG-inducible P_{tac} promoter at a neutral *att* site in the Pf0-1Δ*lapG*Δ*lapD dvhA-hlx-swap* strain along with a *lacI* repressor gene (Fig. 3*A*). Fluorescence intensity of a band at the expected ~75 kDa in a whole-cell lysate western blot showed that DvhD was expressed in the presence of 0.01% IPTG but not without the inducer (Fig. 3*B*). This strain was transformed with pMQ72-*dvhG* or empty pMQ72 as a control, thus allowing us to induce expression of both DvhG (with 0.2% arabinose) and DVU1020 (with 0.01% IPTG), and assay how DVU1020 expression impacts DvhG-mediated proteolysis of the DvhA-hlx-swap adhesin.

We performed static biofilm assays under three conditions: where only DvhG is induced (arabinose), DvhG and DVU1020 are induced (arabinose and IPTG) and where neither are induced (no inducer; Fig. 3*C*). An empty vector control strain was used under the same conditions. When only DvhG is induced (arabinose), we observed a decrease in biofilm formation consistent with DvhG-dependent proteolytic activity. However, when both DvhG and DVU1020 are expressed (arabinose and IPTG) we saw a 56% increase in biofilm formation, suggesting DVU1020 decreases DvhG proteolytic activity analogous to the interactions between LapD and LapG. Under these latter conditions the biofilm formed was on par with the no vector and EV positive controls. The dot blot analysis shows that co-expressing DVU1020 with DvhG, recovered DvhA-hlx-swap on the cell surface by 75% compared to the arabinose-only condition, and consequently, the supernatant associated DvhA-hlx-swap decreased by 54% compared to arabinose-only condition (Fig. 3 *D* and *E*). These data suggest that DVU1020 regulates DvhG cleavage of DvhA, likely by impacting the ability of DvhG to target its substrate. Thus, we renamed DVU1020 to DvhD.

Biofilm Recovery Mediated by DvhD Is Driven by c-di-GMP Levels. The biofilm assays above were performed in a medium with 1 mM added phosphate (abbreviated here as Pi) called K10T-1, which was previously shown to stimulate Pf0-1 biofilm formation. Conversely, when Pi levels are reduced to ~0.1 mM, Pf0-1 induces the expression of the gene encoding the c-di-GMP degrading PDE called RapA. Expression of RapA decreases intracellular c-di-GMP levels and in turn reduces the pool of c-di-GMP to bind to LapD, resulting in the loss of LapA from the cell surface (36). To test whether the rescue in biofilm formation by expressing DvhD is driven by cellular c-di-GMP levels, we manipulated intracellular c-di-GMP concentrations by modulating Pi concentration in the medium and by mutating the *rapA* gene.

We performed static biofilm assays with both DvhD and DvhG induction, DvhG-only induction, and EV control in K10Tπ medium (low phosphate medium, ~0.1 mM; associated with low c-di-GMP) or with high extracellular phosphate (K10T medium, 1 mM, associated with relatively high c-di-GMP). We observed that the growth of Pf0-1 was only modestly reduced in mid-log phase but there was no difference in final yield when extracellular Pi levels were low (*SI Appendix*, Fig. S7). Using these experimental conditions, we calculated the "Δ" which represents the difference in biofilm formed by the strain expressing both DvhG and DvhD (induction with both arabinose and IPTG) and biofilm formation by the strain expressing DvhG but not DvhD (induction with arabinose only). We used this Δ value to account for the differences in baseline biofilm formation in low versus high phosphate; thus, we cannot simply use total biofilm formed in our analysis. Our results indicate that Δ for high Pi condition is 0.5 ± 0.14, which is significantly larger than low Pi condition 0.12 ± 0.044 (Fig. 4*A* and *SI Appendix*, Fig. S8*A*). These data indicate that DvhD inhibition of DvhG activity coincides with intracellular c-di-GMP levels.

Next, we made a markerless *rapA* deletion mutation yielding the Pf0-1 att::*lac*IP$_{tac}$*dvhD*-HA Δ*lapG*Δ*lapD*Δ*rapA dvhA-hlx-swap* strain. In low Pi conditions, when RapA is typically activated and c-di-GMP hydrolyzed, a Δ*rapA* strain should not affect the c-di-GMP levels (36). Conversely, we also constructed a strain in

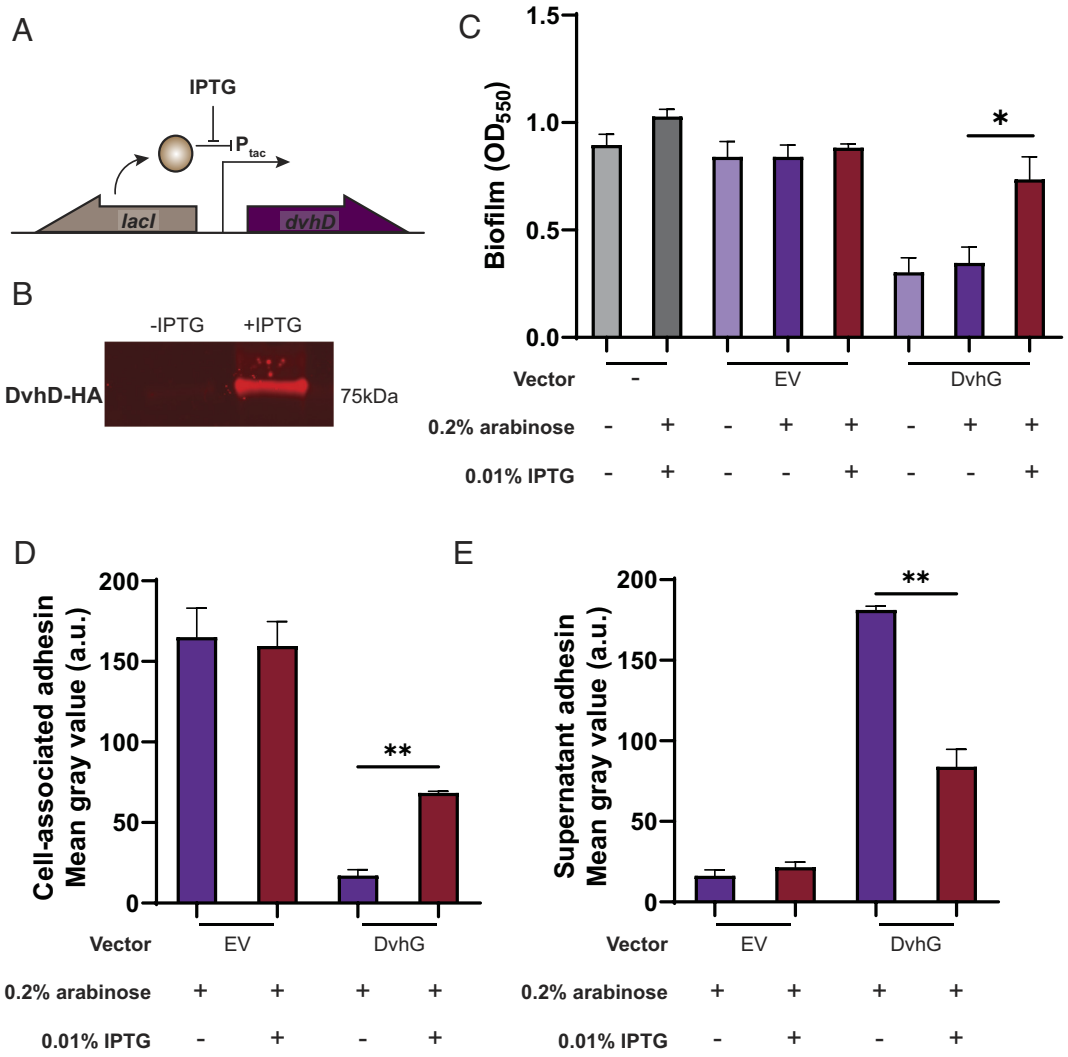

Fig. 3. DvhD rescues the biofilm phenotype of Pf0-1. (*A*) The gene encoding HA-tagged DvhD gene from *D. vulgaris* Hildenborough was inserted at the *Tn7 att* site under the control of IPTG-inducible P_{tac} promoter in the Pf0-1 *ΔlapGΔlapDdvhA-hlx-swap* strain. The *lacI* gene was also introduced at the *att* site to repress *dvhD* gene expression in the absence of IPTG. The diagram depicts the regulatory control of *dvhD* expression. (*B*) Whole-cell western blot for HA-tagged proteins shows minimal DvhD without IPTG and robust DvhD level in the presence of IPTG. (*C*) Biofilm formed by the Pf0-1 attTn7::*lacI*-P_{tac}*dvhD*-HA *ΔlapGΔlapDdvhA-hlx-swap* strain in K10T medium at 24 h. Quantification was performed on the strain containing no vector, empty vector and plasmid expressing full-length DvhG. Arabinose at 0.2% and IPTG at 0.01% were used to induce *dvhG* expression from the plasmid and *dvhD* expression from the genome, respectively. (*D* and *E*) Quantification of DvhA-hlx-swap on the cell surface (*D*) and the culture supernatant (*E*) using dot blots in the presence or absence of IPTG. The analyzed strains carried either an empty vector or a plasmid expressing full-length DvhG, all under inducing conditions with 0.2% arabinose. Statistical analysis was performed using one-way ANOVA corrected for multiple comparisons (ns, $P > 0.05$; *$P \leq 0.05$; **$P \leq 0.01$; ***$P \leq 0.001$; ****$P \leq 0.0001$).

which we placed the *rapA* gene under the control of a xylose-inducible promoter. Induction with xylose under low Pi conditions is expected to increase the level of RapA and drive the intracellular c-di-GMP levels lower than WT. We transformed pMQ72-*dvhG* and EV in these backgrounds and tested for biofilm formation in the low Pi medium and compared conditions with both DvhD and DvhG induction, DvhG-only induction, and EV control (Fig. 4*B*). RapA overexpression was induced with 0.15% xylose.

While we consistently observed higher Δ values in the biofilm formed by the *rapA* deletion strain (0.19 ± 0.11) than in the strain with an active RapA (0.13 ± 0.02), these differences were not significantly different (Fig. 4*B* and *SI Appendix*, Fig. S8*B*). On the other hand, we observed lower Δ values when RapA was expressed under the control of the xylose promoter (0.07 ± 0.01) compared to when WT RapA levels were produced. However, the difference was also not significant.

We then quantified the levels of intracellular c-di-GMP using a P_{cdrA} promoter fused to GFP (Fig. 4*C*). We observe a significant positive association between c-di-GMP level and biofilm formed (R^2= 0.81; P = 0.007). These data show that altering c-di-GMP in this heterologous background results in the expected outcome (low c-di-GMP→low biofilm, high c-di-GMP→high biofilm) for a c-di-GMP-responsive system.

To determine whether DvhD is indeed a c-di-GMP-binding protein, we purified the protein's entire cytoplasmic fragment comprising its PAS and HD-GYP domains and measured its binding of this second messenger. Using isothermal titration calorimetry (ITC), an affinity of 322 ± 81 nM was determined for the interaction between the purified protein fragment and c-di-GMP (Fig. 4*D*). The data confirm a direct, high-affinity interaction between DvhD and c-di-GMP.

Discussion

In this study, we characterize the post-translational regulation of a large adhesive protein important for biofilm formation in *D. vulgaris* Hildenborough (DvH). Our bioinformatic analysis along with work from De Leon et al. revealed T1SS machinery, a

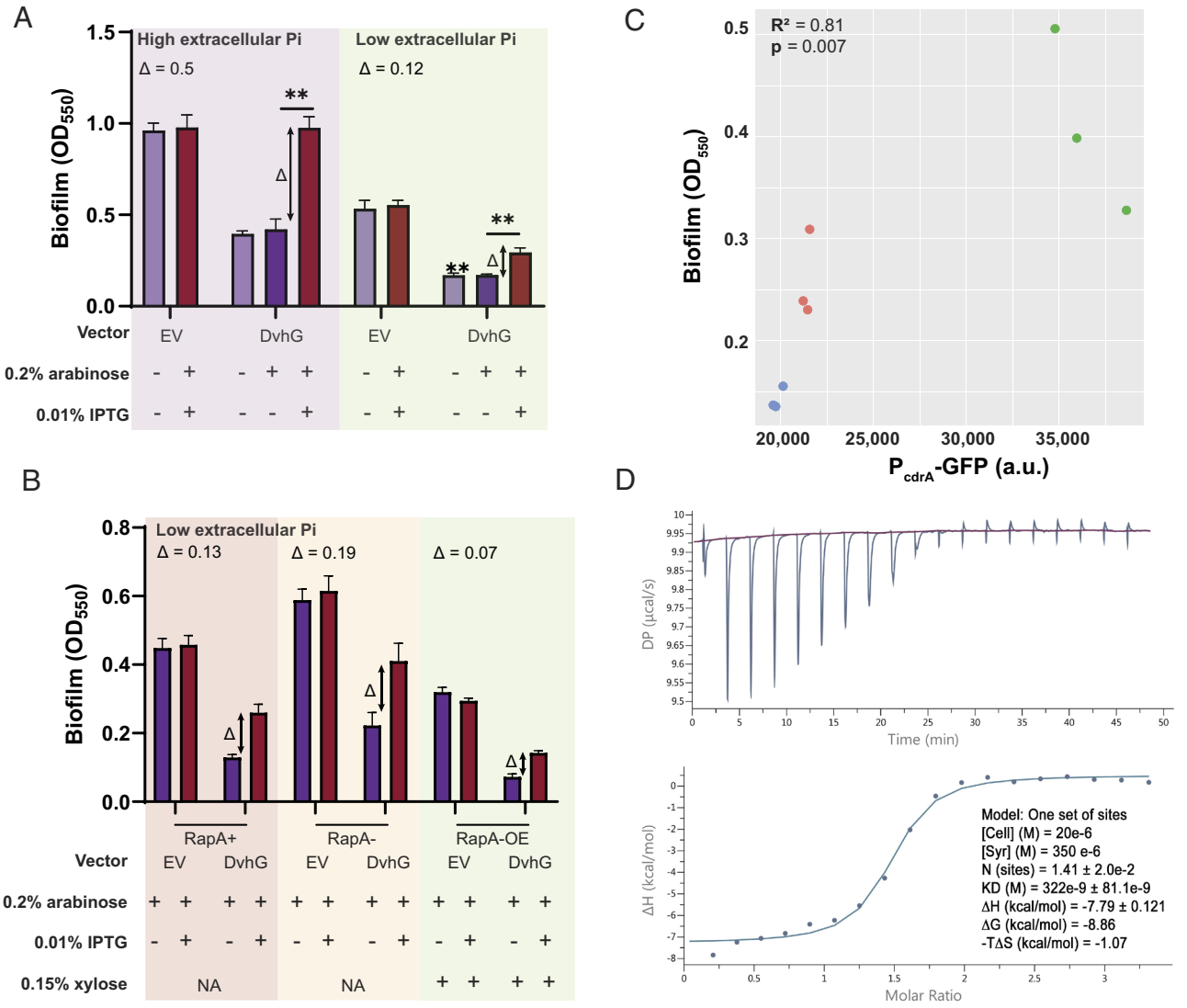

Fig. 4. Biofilm rescue by DvhD is c-di-GMP dependent. (*A*) Biofilm formed in the Pf0-1 attTn7::*lacI*P_{tac}*dvhD*-HA *ΔlapGΔlapDdvhA-hlx-swap* strain in low phosphate K10Tπ medium (~0.1 mM) or high phosphate K10T medium (1 mM) at 24 h. The strain contains either no vector, an empty vector or a plasmid expressing full-length DvhG. Arabinose at 0.2% concentration and IPTG at 0.01% concentration are used to induce *dvhG* expression from the plasmid and *dvhD* expression from the genome, respectively. "Δ" quantifies the extent of biofilm rescue by DvhD and is represented by the difference in biofilm formation by the strain expressing DvhG but not DvhD (purple bar) and biofilm formation by the strain expressing both DvhG and DvhD (red bar). (*B*) Biofilm formed by the Pf0-1 attTn7::*lacI*P_{tac}*dvhD*-HA*ΔlapGΔlapDdvhA-hlx-swap* strain in low phosphate K10Tπ medium at 24 h with, WT RapA phosphodiesterase ($RapA^+$), without $RapA^-$ (Δ*rapA*) or with RapA overexpressed by xylose-inducible P_{xutR} promoter (RapA-OE) in the background. The extent of biofilm rescue by DvhD, "Δ", is compared among the three strains and indicated over the bar plots. Statistical analysis was performed using one-way ANOVA corrected for multiple comparisons (ns, $P > 0.05$; *$P \leq 0.05$; **$P \leq 0.01$; ***$P \leq 0.001$; ****$P \leq 0.0001$). (*C*) Graph representing intracellular c-di-GMP levels calculated from GFP fluorescence from a P_{cdrA}-*gfp* promoter transcriptional fusion plotted versus biofilm formed when DvhD is induced. Linear correlation (R^2) and statistical significance was calculated using Pearson's test in R (v 4.3.0). (*D*) The purified cytosolic fragment of DvhD binds c-di-GMP with high affinity. Isothermal titration calorimetry was used to determine the apparent affinity (expressed as K_D) of DvhD's cytosolic fragment for c-di-GMP. The top graph shows the titration experiment, the bottom graph shows the fit of a single-binding site model to the data. Experimental parameters and calculated binding characteristics are reported in the *Inset*. Shown are representative plots from three independent experiments.

LapG-like protein and large adhesin, similar to the Lap system of *P. fluorescens* Pf0-1 that is critical for biofilm formation. Interesting, DvH lacks an obvious LapD-like homolog.

Here we find that certain aspects of the two Lap systems are functionally similar. The large adhesin DvhA appears to have a retention module at its N terminus and is predicted to be composed of folded beta sheets. The adhesin also shares a highly conserved di-alanine site with LapA, which acts as a target site for proteolysis by DvhG. Like LapG, DvhG is a calcium-dependent cysteine protease that cleaves the large adhesin, leading to a loss of biofilm formation. Further, we identified a protein DvhD that, despite having no domain or sequence similarity to LapD, is functionally analogous to LapD (24) by regulating DvhG activity in response to c-di-GMP and binding c-di-GMP. Previous structural and biochemical studies have shown that LapD can sequester LapG via a conserved tryptophan (Trp) residue, thus preventing the proteolysis of LapA and increasing biofilm formation (39, 40). While we do not have direct evidence yet showing that DvhG interacts with DvhD, we hypothesize that this interaction could be responsible for the biofilm rescue phenotype when we co-express DvhD/DvhG despite the very different periplasmic domains of LapD and DvhD, the latter of which lacks a conserved Trp residue. Last, we also determined that intracellular levels of c-di-GMP contribute to regulating the Lap machinery of DvH, although as outlined below, with some likely differences from the Pf0-1 system.

While there are broad functional similarities between the Pf0-1 and DvH Lap system, we also note some key differences between the two systems. Our results indicate that the proteases LapG and DvhG are highly specific toward their native adhesins and show limited cross-proteolysis in vivo. This finding suggests that the way in which LapA-LapG interact could be distinct from DvhA-DvhG interaction. Sequence analysis of the N terminus of LapA-like adhesins show a conserved residue pair "DP" in addition to the di-alanine motif (22), however, these DP residues are absent in DvhA. While the function of these residues has not been explicitly tested, we hypothesize that they may be responsible for imparting the adhesin's structural specificity toward the proteases.

We also hypothesize that the interaction between DvhG and DvhD is distinct from that characterized for LapD/LapG. As mentioned earlier, in Pf0-1 LapG interacts with LapD via a highly conserved Trp residue in the periplasmic LapD_MoxY_N domain of LapD (39, 40). This residue inserts itself into a hydrophobic binding pocket on the surface of LapG. However, sequence analysis of DvhD shows no conserved Trp residue and no predicted pocket in DvhG. This observation suggests the presence of a distinct interface/residues involved in the DvhG and DvhD interaction. We also note that unlike the periplasmic LapG, DvhG is likely an inner membrane bound protein, which could also affect the mechanics of this interaction.

Furthermore, unlike LapD which has tandem inactive, cytoplasmic GGDEF and EAL domains, DvhD consists of a cytoplasmic HD-GYP domain predicted to be catalytically inactive. We show here that the cytoplasmic portion of DvhD that contains the HD-GYP domain can bind c-di-GMP at high affinity. As DvH is an environmental microbe belonging to the class *deltaproteobacteria,* which are known to have higher fraction of HD-GYP domain containing proteins (41), perhaps this SRB has re-purposed one member of this family of proteins as a c-di-GMP receptor.

Finally, the c-di-GMP network of DvH appears to be complex with 40 DGCs, PDEs and dual domain proteins predicted through sequence analysis (42). This number is almost on par with the Pf0-1 c-di-GMP circuit with 51 proteins (43). However, given the difference in numbers and domains of c-di-GMP sensing proteins (different substrate-binding mechanics/affinities/dynamics) in the two microbes, the dynamics of c-di-GMP regulation, and therefore, the intracellular concentrations of this second messenger could be different. Consistent with this idea, our experiments indicate that DvhD is only partially responsive to changing c-di-GMP levels in Pf0-1. It is worth noting that most of our experiments performed here manipulating c-di-GMP levels were done in low phosphate conditions or by expression or mutation of the RapA PDE. While we know that c-di-GMP levels increase in a Δ*rapA* strain under low phosphate (36), the lack of phosphate is likely affecting other physiological processes that could hamper biofilm formation. Furthermore, our data show that the affinity of the cytoplasmic PAS-HD-GYP domain of DvhD for c-di-GMP in the high nanomolar range. Previously measurements with LapD show affinity to be in the low micromolar range (24, 25). Thus, one caveat of our study is that heterologous expression of DvhD in Pf0-1 may be in the context of a higher range of c-di-GMP concentrations than is typical for DvH, making it more challenging to effectively vary concentrations in the physiological range of DvhD.

Our future work will continue to explore the differences between the two Lap systems. We are especially interested in finding the residues that facilitate binding between DvhG and DvhD, how DvhD regulates DvhG, and the sequences/motifs of DvhA required for DvhG-mediated proteolysis. Finally, beyond DvH, we plan to use Pf0-1 as a chassis to study Lap-like systems of other microbes that may be hard to culture and/or be genetically intractable to broaden our understanding of biofilm formation via these adhesin systems. Such analyses are important because while the Lap-like system is conserved in 1,000+ bacterial genera they are mainly found in the gammaproteobacteria, while the DvH-like systems are mainly restricted to the deltaproteobacteria (*SI Appendix*, Fig. S1*B*). As we identify Lap/Dvh-like systems in other organisms, we can use the *P. fluorescens* Pf0-1 platform to begin to dissect the function of such adhesin systems.

Materials and Methods

Strains and Growth Conditions. *P. fluorescens* Pf0-1 Δ*lapG*Δ*lapD* strain (23) was used as a base strain in the studies here. Mutations were made in this background using *Escherichia coli* S17-1 λpir. Strains used in this study are listed in *SI Appendix*, Table S1. Bacteria were cultured in lysogeny broth (LB) or plated on 1.5% LB agar with antibiotics as needed at 37 °C for *E. coli* and at 30 °C for *P. fluorescens* Pf0-1 (abbreviated Pf0-1). Gentamycin (Gm) was used at a concentration of 10 μg/mL for *E. coli* and at 30 μg/mL for Pf0-1. Carbenicillin (Cb) was used at 100 μg/mL for *E. coli*. Tetracycline (Tet) was used at 15 μg/mL for *E. coli* and 30 μg/mL for Pf0-1. All assays were performed in K10T-1 medium (44): Tris buffer, pH 7.4 (50 mM), Bacto tryptone [0.2% (w/v)], glycerol [0.15% (v/v)], K_2HPO_4 (1 mM), and $MgSO_4$ (0.61 mM). For phosphate-limited conditions, K_2HPO_4 was excluded from K10T-1 medium, yielding K10Tπ, with a phosphate concentration of ~0.1 mM. The medium was assembled from concentrated stock solutions that were either autoclaved (121 °C, 15 min) or filter sterilized. For calcium chelation, K10T-1 was supplemented with 40 μM ethylene glycol-bis(2-aminoethylether)-N, N, N′, N′-tetraacetic acid (EGTA). Genes under the control of the P_{BAD} promoter were induced with arabinose [0.2% (w/v)] and those under P_{tac} promoter were induced with isopropyl-D-thiogalactopyranoside (IPTG, 0.5 mM).

Construction of Plasmids and Mutant Strains. All plasmids and primers used in this study are listed in *SI Appendix*, Tables S1 and S2, respectively. Inserts for plasmid construction were amplified from *D. vulgaris* (strain ATCC 29579/DSM 644/NCIMB 8303/VKM B-1760/Hildenborough) genome. All vectors were assembled with the inserts using Gibson assembly (45). The *lapA-dvhA* adhesin fusions (*dvhA-RM-swap* and *dvhA-hlx-swap*) and *dvhA-hlx-swap* 105PRRG108 were built by allelic exchange using pMQ30 plasmid as described (38, 46). Expression vectors were built using arabinose-inducible pMQ72 vector with genes placed under P_{BAD} promoter. Insertion at the neutral *att* site of Pf0-1 was built using pMQ56 mini-*Tn7* vector with the helper plasmid pUX-BF13. To remove the resistance marker, pFLP3 plasmid was used, followed by sucrose counterselection. Mutations in the *dvhD* gene at the Pf0-1 *att* site were introduced by allelic exchange using pMQ30 plasmid. Pf0-1 *lapB*::pMQ89 was constructed by single-crossover, conferring gentamycin resistance to the strain. All plasmids were constructed in *E. coli* and introduced into Pf0-1 by electroporation, as reported (38).

Static Biofilm Assays. Static biofilm assays were performed as previously described in ref. 36 in K10T-1 or K10Tπ media at 24 h at 30 °C using crystal violet staining. Details of the procedure are described in *SI Appendix, SI Text*.

Quantitative Adhesin Surface Localization Assay Using Dot Blots. Localization of the adhesin was probed with the help of dot blots using Pf0-1 strains with a functional 3×HA-tagged adhesin as described in ref. 36 Briefly, overnight Pf0-1 cultures were subcultured in 5 mL K10T-1 medium (1:100 dilution) and incubated for 24 h. The cultures were OD_{600} normalized and spotted directly on a nitrocellulose membrane. Supernatant samples were prepared by filter-sterilizing the OD_{600} normalized cultures before spotting on the membrane. The blots were probed for the adhesin using α-HA antibodies and chemiluminescence, as reported (36).

Detection and Quantification of Proteins Using Western Blots. Pf0-1 strains with genome-integrated DvhD harboring a functional HA tag or with adhesins harboring 3×-HA tag were used to detect and quantify the proteins. The samples were prepared and processed as described above for dot blots. Pf0-1 strains with 6×-His tagged DvhG (or DvhG variants) on a pMQ72 plasmid were used to detect and quantify this protein. Empty vector pMQ72 was used as a negative control. For all western blots, subcultured samples were normalized for cell density (OD_{600}) and protein content using BCA assay (Pierce). After resolving

the samples on SDS-Page gels and transferring to a nitrocellulose membrane, the proteins were quantified using fluorescence intensity. Detailed procedures of western blots are provided in *SI Appendix, SI Text*.

Bioinformatics Analysis. The Simple Modular Architecture Research Tool (SMART, https://smart.embl-heidelberg.de/) was used to identify LapG- and LapD-like proteins. LapG contains a "Pfam: Peptidase_C93" domain and LapD-like proteins contain a periplasmic "Pfam: LapD_MoxY_N" domain. The SMART Domain selection tool was used to identify proteins in the database containing either domain and the FASTA results were saved for analysis in R. Bacterial species encoding LapG-like and LapD-like were identified using the R "intersect" function and genomes encoding only LapG or LapD were identified using the "setdiff" function. The Bacteria and Viral Bioinformatic Resource Center (https://www.bv-brc.org/) was used to manually inspect the genomic regions surrounding LapG.

Isothermal Titration Calorimetry (ITC). DNA fragments encoding the cytoplasmic portion of DvhD (residues 374 to 701 of DVU1020) were synthesized commercially after computational codon optimization using the preferred codon usage in *E. coli*. Using the SLiCE cloning method (46), DNA fragments were inserted into a modified pET28 bacterial expression plasmid (Novagen) that adds an N-terminal His_6-SUMO purification tag. The protein was recombinantly expressed in *E. coli* BL21DE3 (New England Biolabs), grown in Terrific Broth (TB) medium supplemented with kanamycin. Cultures were grown at 37 °C to an optical density at 600 nm (OD600) of ~0.6 to 0.9, at which point the temperature was shifted to 18 °C and IPTG (0.5 mM final concentration) was added. After overnight induction with IPTG, cells were centrifuged (4,000 × g, 45 min, 4 °C), resuspended in Ni-nitrilotriacetic acid (Ni-NTA) buffer A [25 mM Tris-HCl (pH 7.5), 500 mM NaCl, 20 mM imidazole]. Cell suspensions were lysed by sonication and cell debris was removed by centrifugation (20,000 × g, 45 min at 4 °C). The cleared lysates were incubated with Ni-NTA Superflow resin (Qiagen) that had been pre-equilibrated with Ni-NTA buffer A. The resin was washed with 20 column volumes of buffer A, followed by protein elution with five column volumes of Ni-NTA buffer B [25 mM Tris-HCl (pH 8.5), 500 mM NaCl, and 300 mM imidazole]. The eluate was subjected to buffer exchange into gel filtration buffer [25 mM Tris-HCl (pH 8.5) and 150 mM NaCl] on a fast-desalting column (Cytiva), followed by addition of yeast Ulp-1 to cleave off the His_6-SUMO moiety in an overnight incubation. The cleaved protein was recovered in the flow-through of a second Ni-NTA chromatography step and subjected to size-exclusion chromatography on a Superdex 200 16/600 column (GE Healthcare) preequilibrated with gel filtration buffer [25 mM Tris-HCl (pH 7.5), 150 mM NaCl]. Purified proteins were concentrated on Amicon filters with an appropriate size cutoff to concentrations of >25 mg/mL, flash frozen in liquid nitrogen, and stored at −80 °C.

The ligand (c-di-GMP) was dissolved in gel filtration buffer (350 μM final concentration) and titrated into a solution of the purified cytoplasmic fragment of DvhD (20 μM) using a MicroCal PEAQ-ITC instrument (Malvern Panalytical). Injections of c-di-GMP (first injection: 0.5 μL; subsequent injections: 4 μL; spacing 150 s) were performed at 25 °C. Data were fitted and analyzed using PEAQ software (Malvern Panalytical). A single-site binding model fits the data most optimally, and the apparent binding characteristics were calculated based on this fit.

Protein Structure Prediction. We employed ColabFold (v1.5.5) to generate structural models of the domains of DvhA using AlphaFold2 with default parameters (47, 48). With its 3,038 residues, the DvhA protein sequence is too long to be modeled in a single step. Therefore, the sequence was divided into four segments (S1, residues 1 to 206; S2, residues 207 to 1,110; S3, residues 1,111 to 2,220; S4, residues 2,221 to 3,038). Segments S2 and S3 contain repeating units that were identified using the RADAR algorithm (49) and informed the segmentation of the DvhA sequence. For each segment, five models were generated and ranked by model confidence (pLDDT metric). The top-ranked models of the individual predictions were relaxed by molecular dynamics within ColabFold. Representative domains were illustrated using Pymol (The PyMOL Molecular Graphics System, Version 2.0 Schrödinger, LLC), with domain annotations taken from InterPro (42).

Statistics. Data visualization and statistical analysis were performed in GraphPad Prism 9 (v.9.2.0). Linear models were built in R (v.4.3.0) and visualized using ggplot2 (v.3.4.2). The script used to perform the analyses can be found at https://github.com/GeiselBiofilm.

Data, Materials, and Software Availability. All study data are included in the article and/or *SI Appendix*.

ACKNOWLEDGMENTS. We would like to thank Prof. Will D. Leavitt for providing us with the *D. vulgaris* strain used in this study and helping us kick-start the project. We thank Dr. Thomas Hampton and Kaitlyn Barrack for their help with statistical analysis. We also thank Dr. Sherry Kuchma and Christopher Geiger for thoughtful discussions and help with flow cytometry. This work was supported by NIH grant R01GM123609 G.A.O. This work was also supported by bioMT through NIH NIGMS grant P20-GM113132.

1. H.-C. Flemming, S. Wuertz, Bacteria and archaea on Earth and their abundance in biofilms. *Nat. Rev. Microbiol.* **17**, 247–260 (2019).
2. E. Karatan, P. Watnick, Signals, regulatory networks, and materials that build and break bacterial biofilms. *Microbiol. Mol. Biol. Rev.* **73**, 310–347 (2009).
3. H.-C. Flemming *et al.*, The biofilm matrix: Multitasking in a shared space. *Nat. Rev. Microbiol.* **21**, 70–86 (2023).
4. U. Römling, Cyclic di-GMP signaling–Where did you come from and where will you go? *Mol. Microbiol.* **120**, 564–574 (2023).
5. M. Stylo, N. Neubert, Y. Roebbert, S. Weyer, R. Bernier-Latmani, Mechanism of uranium reduction and immobilization in *Desulfovibrio vulgaris* biofilms. *Environ. Sci. Technol.* **49**, 10553–10561 (2015).
6. Y. Park, D. Faivre, Diversity of microbial metal sulfide biomineralization. *ChemPlusChem* **87**, e202100457 (2022).
7. D. R. Lovley, Electrotrophy: Other microbial species, iron, and electrodes as electron donors for microbial respirations. *Bioresour. Technol.* **345**, 126553 (2022).
8. C. Diao *et al.*, Application of microbial sulfate-reduction process for sulfate-laden wastewater treatment: A review. *J. Water Process Eng.* **52**, 103537 (2023).
9. I. C. B. Rodrigues, V. A. Leão, Producing electrical energy in microbial fuel cells based on sulphate reduction: A review. *Environ. Sci. Pollut. Res.* **27**, 36075–36084 (2020).
10. J. Telegdi, A. Shaban, L. Trif, "8 - microbiologically influenced corrosion (MIC)" in *Trends in Oil and Gas Corrosion Research and Technologies*, *Woodhead Publishing Series in Energy*, A. M. El-Sherik, Ed. (Woodhead Publishing, 2017), pp. 191–214.
11. T. Ueki, D. R. Lovley, *Desulfovibrio vulgaris* as a model microbe for the study of corrosion under sulfate-reducing conditions. *mLife* **1**, 13–20 (2022).
12. G. Scarascia *et al.*, Effect of quorum sensing on the ability of *Desulfovibrio vulgaris* to form biofilms and to biocorrode carbon steel in saline conditions. *Appl. Environ. Microbiol.* **86**, e01664-19 (2019).
13. W. Zhang, D. E. Culley, L. Nie, J. C. M. Scholten, Comparative transcriptome analysis of *Desulfovibrio vulgaris* grown in planktonic culture and mature biofilm on a steel surface. *Appl. Microbiol. Biotechnol.* **76**, 447–457 (2007).
14. M. E. Clark, R. E. Edelmann, M. L. Duley, J. D. Wall, M. W. Fields, Biofilm formation in *Desulfovibrio vulgaris* Hildenborough is dependent upon protein filaments. *Environ. Microbiol.* **9**, 2844–2854 (2007).
15. M. E. Clark *et al.*, Transcriptomic and proteomic analyses of *Desulfovibrio vulgaris* biofilms: Carbon and energy flow contribute to the distinct biofilm growth state. *BMC Genomics* **13**, 138 (2012).
16. P. J. Walian *et al.*, High-throughput isolation and characterization of untagged membrane protein complexes: Outer membrane complexes of *Desulfovibrio vulgaris*. *J. Proteome Res.* **11**, 5720–5735 (2012).
17. B. Han *et al.*, Survey of large protein complexes in *D. vulgaris* reveals great structural diversity. *Proc. Natl. Acad. Sci. U.S.A.* **106**, 16580–16585 (2009).
18. K. B. De León *et al.*, Unintended laboratory-driven evolution reveals genetic requirements for biofilm formation by *Desulfovibrio vulgaris* Hildenborough. *mBio* **8**, e01696-17 (2017).
19. T. J. Smith, H. Sondermann, G. A. O'Toole, Type 1 does the two-step: Type 1 secretion substrates with a functional periplasmic intermediate. *J. Bacteriol.* **200**, e00168-18 (2018), 10.1128/jb.00168-18.
20. A. J. Collins, T. J. Smith, H. Sondermann, G. A. O'Toole, From input to output: The Lap/c-di-GMP biofilm regulatory circuit. *Annu. Rev. Microbiol.* **74**, 607–631 (2020).
21. S. Guo *et al.*, Structure of a 1.5-MDa adhesin that binds its Antarctic bacterium to diatoms and ice. *Sci. Adv.* **3**, e1701440 (2017).
22. T. J. Smith, M. E. Font, C. M. Kelly, H. Sondermann, G. A. O'Toole, An N-terminal retention module anchors the giant adhesin LapA of *Pseudomonas fluorescens* at the cell surface: A novel subfamily of Type I secretion systems. *J. Bacteriol.* **200**, e00734-17 (2018).
23. P. D. Newell, C. D. Boyd, H. Sondermann, G. A. O'Toole, A c-di-GMP effector system controls cell adhesion by inside-out signaling and surface protein cleavage. *PLoS Biol.* **9**, e1000587 (2011).
24. P. D. Newell, R. D. Monds, G. A. O'Toole, LapD is a bis-(3′,5′)-cyclic dimeric GMP-binding protein that regulates surface attachment by *Pseudomonas fluorescens* Pf0-1. *Proc. Natl. Acad. Sci. U.S.A.* **106**, 3461–3466 (2009).
25. M. V. A. S. Navarro *et al.*, Structural basis for c-di-GMP-mediated inside-out signaling controlling periplasmic proteolysis. *PLoS Biol.* **9**, e1000588 (2011).
26. M. Gjermansen, M. Nilsson, L. Yang, T. Tolker-Nielsen, Characterization of starvation-induced dispersion in *Pseudomonas putida* biofilms: Genetic elements and molecular mechanisms. *Mol. Microbiol.* **75**, 815–826 (2010).
27. N. Ambrosis, C. D. Boyd, G. A. O'Toole, J. Fernández, F. Sisti, Homologs of the LapD-LapG c-di-GMP effector system control biofilm formation by Bordetella bronchiseptica. *PLoS One* **11**, e0158752 (2016).
28. M. Rybtke *et al.*, The LapG protein plays a role in *Pseudomonas aeruginosa* biofilm formation by controlling the presence of the CdrA adhesin on the cell surface. *MicrobiologyOpen* **4**, 917–930 (2015).

29. D. Chatterjee, C. D. Boyd, G. A. O'Toole, H. Sondermann, Structural characterization of a conserved, calcium-dependent periplasmic protease from *Legionella pneumophila*. *J. Bacteriol.* **194**, 4415–4425 (2012).
30. C. D. Boyd *et al.*, Structural features of the *Pseudomonas fluorescens* biofilm adhesin LapA required for LapG-dependent cleavage, biofilm formation, and cell surface localization. *J. Bacteriol.* **196**, 2775–2788 (2014).
31. M. Y. Galperin, S.-H. Chou, Sequence conservation, domain architectures, and phylogenetic distribution of the HD-GYP Type c-di-GMP phosphodiesterases. *J. Bacteriol.* **204**, e00561-21 (2022).
32. J. F. Heidelberg *et al.*, The genome sequence of the anaerobic, sulfate-reducing bacterium *Desulfovibrio vulgaris* Hildenborough. *Nat. Biotechnol.* **22**, 554–559 (2004).
33. K. L. Keller, K. S. Bender, J. D. Wall, Development of a markerless genetic exchange system for *Desulfovibrio vulgaris* Hildenborough and its use in generating a strain with increased transformation efficiency. *Appl. Environ. Microbiol.* **75**, 7682–7691 (2009).
34. J. D. Wall *et al.*, Deletion mutants, archived transposon library, and tagged protein constructs of the model sulfate-reducing bacterium *Desulfovibrio vulgaris* Hildenborough. *Microbiol. Resour. Announc.* **10**, e00072-21 (2021), 10.1128/mra.00072-21.
35. C. D. Boyd, D. Chatterjee, H. Sondermann, G. A. O'Toole, LapG, required for modulating biofilm formation by *Pseudomonas fluorescens* Pf0-1, is a calcium-dependent protease. *J. Bacteriol.* **194**, 4406–4414 (2012).
36. R. D. Monds, P. D. Newell, R. B. Gross, G. A. O'Toole, Phosphate-dependent modulation of c-di-GMP levels regulates *Pseudomonas fluorescens* Pf0-1 biofilm formation by controlling secretion of the adhesin LapA. *Mol. Microbiol.* **63**, 656–679 (2007).
37. K. Ginalski, L. Kinch, L. Rychlewski, N. V. Grishin, BTLCP proteins: A novel family of bacterial transglutaminase-like cysteine proteinases. *Trends Biochem. Sci.* **29**, 392–395 (2004).
38. R. M. Q. Shanks, N. C. Caiazza, S. M. Hinsa, C. M. Toutain, G. A. O'Toole, *Saccharomyces cerevisiae*-based molecular tool kit for manipulation of genes from gram-negative bacteria. *Appl. Environ. Microbiol.* **72**, 5027–5036 (2006).
39. D. Chatterjee *et al.*, Mechanistic insight into the conserved allosteric regulation of periplasmic proteolysis by the signaling molecule cyclic-di-GMP. *eLife* **3**, e03650 (2014).
40. R. B. Cooley, J. P. O'Donnell, H. Sondermann, Coincidence detection and bi-directional transmembrane signaling control a bacterial second messenger receptor. *eLife* **5**, e21848 (2016).
41. M. Y. Galperin, S. Chou, Sequence conservation, domain architectures, and phylogenetic distribution of the HD-GYP Type c-di-GMP phosphodiesterases. *J. Bacteriol.* **204**, e00561-21 (2021).
42. T. Paysan-Lafosse *et al.*, InterPro in 2022. *Nucleic Acids Res.* **51**, D418–D427 (2023).
43. K. M. Dahlstrom *et al.*, A multimodal strategy used by a large c-di-GMP network. *J. Bacteriol.* **200**, e00703-17 (2018).
44. R. D. Monds, P. D. Newell, J. A. Schwartzman, G. A. O'Toole, Conservation of the Pho regulon in *Pseudomonas fluorescens* Pf0-1. *Appl. Environ. Microbiol.* **72**, 1910–1924 (2006).
45. D. G. Gibson *et al.*, Enzymatic assembly of DNA molecules up to several hundred kilobases. *Nat. Methods* **6**, 343–345 (2009).
46. Y. Zhang, U. Werling, W. Edelmann, SLiCE: A novel bacterial cell extract-based DNA cloning method. *Nucleic Acids Res.* **40**, e55 (2012).
47. J. Jumper *et al.*, Highly accurate protein structure prediction with AlphaFold. *Nature* **596**, 583–589 (2021).
48. M. Mirdita *et al.*, ColabFold: Making protein folding accessible to all. *Nat Methods* **19**, 679–682 (2022).
49. A. Heger, L. Holm, Rapid automatic detection and alignment of repeats in protein sequences. *Proteins: Struc., Funct., Bioinform.* **41**, 224–237 (2000).